Benzofuroxane Derivatives as Multi-Effective Agents for the Treatment of Cardiovascular Diabetic Complications. Synthesis, Functional Evaluation, and Molecular Modeling Studies

Stefania Sartini,[†] Sandro Cosconati,[§] Luciana Marinelli,*[‡] Elisabetta Barresi,[†] Salvatore Di Maro,[‡] Francesca Simorini,[†] Sabrina Taliani,[†] Silvia Salerno,[†] Anna Maria Marini,[†] Federico Da Settimo,[†] Ettore Novellino,[‡] and Concettina La Motta*[†]

[†]Dipartimento di Farmacia, Università di Pisa, Via Bonanno 6, 56126 Pisa, Italy

[‡]Dipartimento di Chimica Farmaceutica e Tossicologica, Università di Napoli "Federico II", Via D. Montesano, 49, 80131 Napoli, Italy

[§]Dipartimento Scienze e Tecnologie Ambientali, Biologiche e Farmaceutiche, Seconda Università di Napoli, Via Vivaldi 43, 81100 Caserta, Italy

S *Supporting Information*

ABSTRACT: Diabetes mellitus is the major risk factor for cardiovascular disorders. Aldose reductase, the rate-limiting enzyme of the polyol pathway, plays a key role in the pathogenesis of diabetic complications. Accordingly, inhibition of this enzyme is emerging as a major therapeutic strategy for the treatment of hyperglycemia-induced cardiovascular pathologies. In this study, we describe a series of 5(6)-substituted benzofuroxane derivatives, **5a−k,m**, synthesized as aldose reductase inhibitors. Besides inhibiting efficiently the target enzyme, **5a−k,m** showed additional NO donor and antioxidant properties, thus emerging as novel multi-effective compounds. The benzyloxy derivative **5a**, the most promising of the whole series, showed a well-balanced, multifunctional profile consisting of submicromolar ALR2 inhibitory efficacy (IC$_{50}$ = 0.99 ± 0.02 μM), significant and spontaneous NO generation properties, and excellent hydroxyl radical scavenging activity. Computational studies of the novel compounds clarified the aldose reductase inhibitory profile observed, thus rationalizing structure−activity relationships of the whole series.
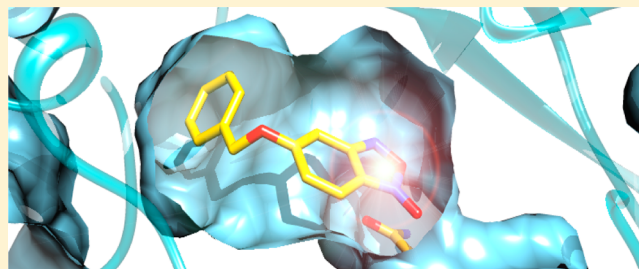
High Inhibitory Potency, NO Donor & Antioxidant Properties

INTRODUCTION

Diabetes mellitus is a complex and chronic metabolic disorder now recognized as a public health problem, as it affects a significant portion of the population worldwide and is expanding to pandemic dimensions. Actually, according to epidemiological data, 366 million people were diagnosed with diabetes in 2011, but this number is expected to rise sharply to 552 million people within the next 20 years.[1−3] The economic cost attributable to the management of this disease markedly influences countries' health budgets, being the highest of any disease category. In 2011, the United States paid $465 billion, 11% of total healthcare expenditures for adults aged 20−79 years, to hold up not only direct costs of diabetes care but also indirect costs of both short-term or permanent disability and of premature retirement or death.[4] Indeed, although diabetes can be successfully controlled by the administration of potent hypoglycemics and/or insulin, it still remains the cause of significant morbidity and mortality, because of the progressive development of microvascular and macrovascular alterations. In particular, according to the Scientific Advisory and Coordinating Committee of the American Heart Association, diabetes is the major risk factor for cardiovascular disorders, and people with chronic hyperglycemia are 2−4 times more likely to have a heart attack, coronary artery diseases, peripheral arterial diseases, cardiomyopathy, angina, and endothelial disfunction than people without diabetes.[5]

Many hypotheses have been proposed to explain the pathogenic mechanism leading to diabetic complications. These include nonenzymatic glycation of proteins, alteration of myoinositol levels, impairment of antioxidant defense, mitochondrial respiratory chain disruption, and activation of both the hexosamine pathway and protein kinase C isoforms.[6−9] However, the prominent theory suggests that they are causally linked to an increased flux of glucose through the polyol pathway, ruled by aldose reductase (alditol:NADP⁺ oxidoreductase, EC 1.1.1.21, ALR2), a monomeric enzyme belonging to the aldo-keto reductase (AKR) superfamily.[10] ALR2 drains away the excess of glucose, catalyzing its reduction to sorbitol, but the resulting polyol, slowly oxidized to fructose
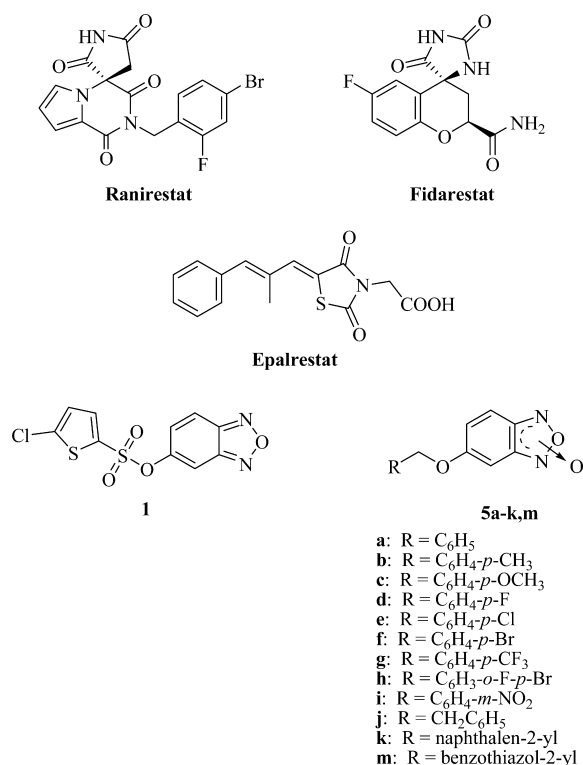
by the NAD$^+$-dependent sorbitol dehydrogenase, tends to accumulate inside the cells, thus increasing cellular osmolarity. In addition to the osmotic imbalance, ALR2 activation causes a marked impairment of the NADPH/NADP$^+$ free cytosolic coenzyme ratio, thus inducing a state of pseudohypoxia that promotes the onset of hyperglycemic oxidative stress through the accumulation of reactive oxygen species (ROS). Moreover, as the increased flux of glucose through the polyol pathway is closely related to myoinositol depletion, protein kinase C (PKC) activation, and nonenzymatic protein glycation, ALR2 can clearly be identified as the key and critical checkpoint for the main pathological changes associated with long-term diabetic complications. Hence, ALR2 represents an excellent drug target, as its inhibition can significantly minimize the onset of osmotic and oxidative stress, as well as the activation of other downstream biochemical pathways, making it possible to prevent, or at least delay, the progression and severity of diabetic complications.[11,12]

A huge amount of experimental data, gathered in the decades since the discovery of ALR2, clearly proved the effectiveness of ALR2 inhibitors (ARIs) in treating hyperglycemia-induced pathologies like neuropathy, nephropathy, retinopathy, and cataract. The main examples of active compounds are represented by either spiro derivatives, like fidarestat[13] and ranirestat[14] (Chart 1), presently undergoing clinical trials in

Chart 1. Aldose Reductase Inhibitors

Ranirestat

Fidarestat

Epalrestat

1

5a–k,m

a: R = C$_6$H$_5$
b: R = C$_6$H$_4$-p-CH$_3$
c: R = C$_6$H$_4$-p-OCH$_3$
d: R = C$_6$H$_4$-p-F
e: R = C$_6$H$_4$-p-Cl
f: R = C$_6$H$_4$-p-Br
g: R = C$_6$H$_4$-p-CF$_3$
h: R = C$_6$H$_3$-o-F-p-Br
i: R = C$_6$H$_4$-m-NO$_2$
j: R = CH$_2$C$_6$H$_5$
k: R = naphthalen-2-yl
m: R = benzothiazol-2-yl

both the United States and Asia, or acetic acid compounds, such as epalrestat (Chart 1), which is currently marketed for the treatment of diabetic neuropathy but is also able to prevent the progression of both retinopathy and nephropathy.[15,16]

More recently, a growing body of compelling evidence is demonstrating that ALR2 also plays a pivotal role in the development of diabetic cardiomyopathy, atherosclerosis, hypertension, restenosis, angiopathy, and endothelial dysfunc-

tions. Accordingly, a novel and still unexplored scenario is being elucidated for the use of ARIs, which could be profitably exploited for the effective treatment of people affected by hyperglycemia-induced cardiovascular diseases.[17−22]

Our research group has been involved in the development of novel ARIs for many years, to identify a drug candidate for the treatment of long-term diabetic complications.[23−31] Through a virtual screening (VS) campaign, performed by integrating a receptor-based approach with a ligand-based one, we recently disclosed a number of viable chemical entities that deserve further examination in the search for potent ALR2 inhibitors.[25] Among the discovered hits, the benzo[c][1,2,5]oxadiazole derivative KM07100 [**1** (Chart 1); IC$_{50}$ = 35.6 ± 1.8 μM] emerged as the most intriguing candidate, being characterized by an unusual core, never exploited before in the ARI field. This scaffold was predicted to be lodged in the enzyme anion binding site H-bonding to the Y48, H110, and W111 residues, which have been demonstrated to be contacted by the carboxylic and hydantoin groups of the most active ARIs described so far. However, different from the previously described ARIs, the benzo[c][1,2,5]oxadiazole scaffold should not pose, in principle, the risk of failure shown by most ARIs described in the literature that, although promising during in vitro studies or in trials with animal models, often fail to proceed any further, because of either pharmacokinetic restrictions, typical of inhibitors bearing a carboxylic function, or unwanted side effects, arising with the use of hydantoinic-like inhibitors. Prompted by this speculation, we embarked in a hit to lead optimization campaign and focused our attention on the benzo[c][1,2,5]oxadiazole synthetic precursor, benzofuroxane, exploited previously by different authors for its pharmacological properties.[32−34]

Actually, the well-known NO donor, vasorelaxant, and platelet anti-aggregating activities of the benzofuroxane core made this scaffold more appealing than the parent benzoxadiazole. As experimental data clearly prove, most of the diabetic complications affecting the cardiovascular system result from an impaired endothelium-derived NO production and action.[35,36] Accordingly, a NO donor compound should certainly represent a privileged structure in the search for a novel drug candidate for the treatment of diabetes-related cardiovascular diseases. In addition, the hypoglycemic/anti-hyperglycemic effect of NO might help to control blood glucose levels, while its anti-aggregating properties could profitably counterbalance platelet aggregation observed under hyperglycemic conditions. Moreover, as demonstrated by Srivastava and co-workers, endogenous NO is able to regulate ALR2 activity, as it may inactivate enzyme catalytic function by inducing a reversible glutathiolation of the highly reactive residue C298, located at the ALR2 active site. Therefore, increasing the intracellular levels of NO may certainly contribute to keeping the enzyme in a partially inhibited state, thus controlling or even preventing pathological changes triggered by ALR2.[37−40]

The choice of the benzofuroxane ring was also suggested by the necessity of enhancing the interactions of the new ARIs with the enzyme anion binding site. In fact, preliminary profiling of the electrostatic potential through ab initio calculations demonstrated that the benzofuroxane scaffold should be more electron-rich than the parent benzo[c][1,2,5]-oxadiazole one, thus being more prone to establishing tight interactions with the aforementioned ALR2 region (Figure 1a). Moreover, a preliminary docking study of N-oxide derivative **5a**
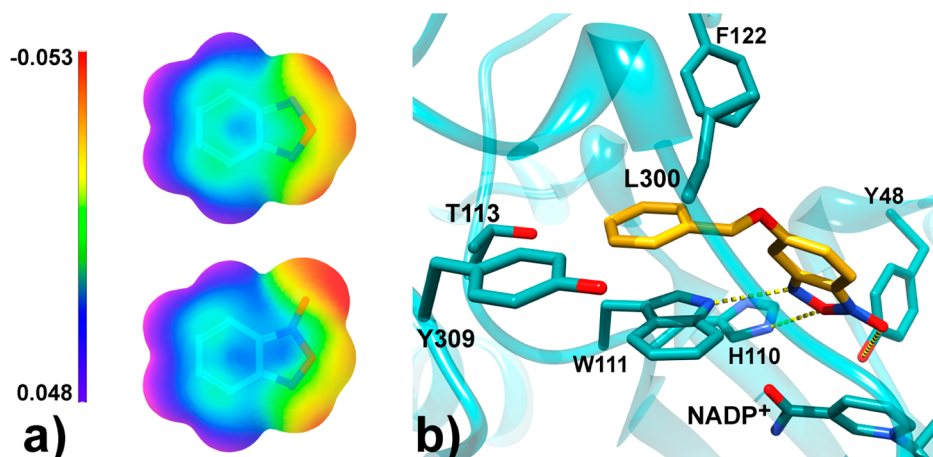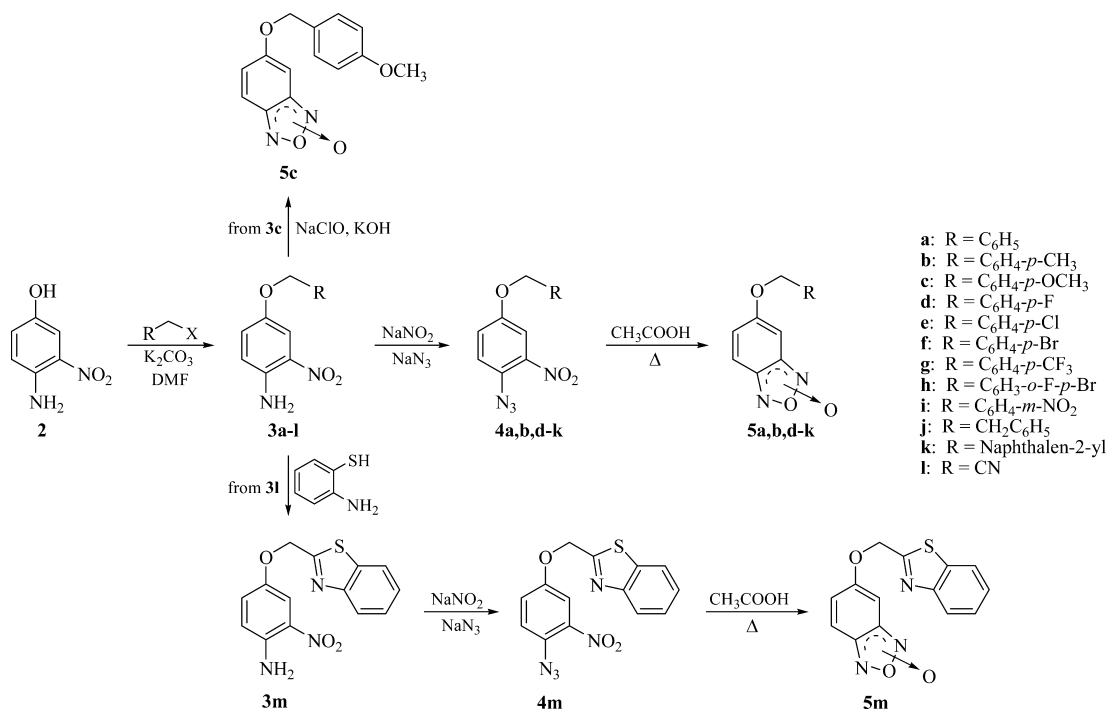
Figure 1. ALR2 and ALR1 inhibition data and predicted binding free energies of benzofuroxane derivatives **5a–k,m**.

Scheme 1. Synthesis of Benzofuroxane Derivatives 5a–k,m

in the ALR2 active site revealed that the benzofuroxane scaffold should be able to engage in well-oriented H-bond interactions with the side chains of W111, H110, and Y48 in the protein anion binding pocket, while its benzyloxy pendant chain is lodged in the specificity pocket forming a π–π stacking interaction with W111 and hydrophobic contacts with F122, L300, and Y309 (Figures 1b and Figures S1 and S2 of the Supporting Information). Analogous results were also achieved when docking was performed explicitly considering water molecules during docking calculations employing the newly described method of Forli and Olson (Figure S3 of the Supporting Information).[41] These encouraging theoretical data led us to move, once and for all, to the benzofuroxane core as a viable candidate in the search for noncarboxylic, non-hydantoinic, ALR2 inhibitors.

In this work, we present the synthesis of the novel benzofuroxane derivatives, **5a–k,m** (Chart 1), whose benzo-fused ring was suitably substituted through the insertion of aromatic and lipophilic groups. These latter groups were chosen among the ones already borne by well-known ARIs from the literature, to plainly comply with pharmacophore requirements of the ALR2 binding site.[42] All the synthesized compounds were extensively evaluated for their functional effectiveness, testing their ALR2 inhibitory activity and selectivity, as well as their ability to generate NO and efficacy in scavenging reactive oxygen species (ROS). Moreover, simulations of docking of the test compounds into the human ALR2 binding site were carried out, to rationalize structure–activity relationships (SARs) observed and to guide, prospectively, the development of more effective analogues.
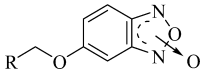
■ CHEMISTRY

The target inhibitors, **5a–k,m** were obtained as outlined in Scheme 1, according to synthetic methods previously reported in the literature. Chemoselective alkylation of the commercially available 4-amino-3-nitrophenol, **2**, performed with the suitable

alkyl halide in the presence of anhydrous potassium carbonate, gave the 4-substituted 2-nitrobenzenamine derivatives 3a–l.[43] Reaction of 3a,b,d–k with sodium nitrite and sodium azide led to the corresponding azide intermediates, 4a,b,d–k, respectively, which afforded target inhibitors, 5a,b,d–k, respectively, through reaction with refluxing acetic acid.[44] Compound 3c, bearing a 4-methoxybenzyloxy substituent, gave inhibitor 5c through the Green–Rowe oxidative cyclization, performed with sodium hypochlorite in a basic alcoholic solution.[45] Derivative 3l, carrying a 4-cyanomethoxy group, was treated with 2-aminobenzenethiol, and the resulting 4-(benzo[d]thiazol-2-ylmethoxy)-2-nitrobenzenamine, 3m, provided the key intermediate 4m through reaction with sodium nitrite and sodium azide. Cyclization of 4m, performed with refluxing acetic acid, led to the desired 5m.

■ RESULTS AND DISCUSSION

Functional Evaluation. We started our functional evaluation by testing the synthesized inhibitors, 5a–k,m, for their efficacy against ALR2. As reported in Table 1, in which

Table 1. ALR2 and ALR1 Inhibition Data and Predicted Binding Free Energies of Benzofuroxane Derivatives 5a–k,m

N	R	ALR2 IC$_{50}$ (μM)^a	ALR1 IC$_{50}$ (μM) or % inhibition	ΔG_{AD4} (kcal/mol)
1		35.6 ± 1.80	20 ± 0.9^b	
5a	C$_6$H$_5$	0.99 ± 0.02	26 ± 1.2^b	−7.10
5b	C$_6$H$_4$-4-CH$_3$	0.83 ± 0.03	24 ± 0.8^b	−7.47
5c	C$_6$H$_4$-4-OCH$_3$	4.52 ± 0.19	na^c	−7.62
5d	C$_6$H$_4$-4-F	0.82 ± 0.02	na^c	−7.14
5e	C$_6$H$_4$-4-Cl	0.92 ± 0.04	19 ± 0.9^b	−7.50
5f	C$_6$H$_4$-4-Br	7.36 ± 0.37	19 ± 0.7^b	−6.94
5g	C$_6$H$_4$-4-CF$_3$	1.94 ± 0.61	14^b	−7.09
5h	C$_6$H$_4$-2-F-4-Br	1.41 ± 0.05	na^c	−7.85
5i	C$_6$H$_4$-3-NO$_2$	0.46 ± 0.01	5 ± 0.2^b	−7.33
5j	CH$_2$-C$_6$H$_5$	5.90 ± 0.25	11 ± 0.4^b	−7.25
5k	naphthalen-2-yl	1.43 ± 0.04	35 ± 1.6^b	−8.20
5m	benzothiazol-2-yl	0.42 ± 0.01	38 ± 1.8^b	−7.96
epalrestat		0.17 ± 0.01	0.94 ± 0.04^a	

^{a}IC$_{50}$ values (means ± standard deviation) represent the concentration required to produce 50% enzyme inhibition. ^{b}Percent of ALR1 inhibition determined at 100 μM. ^{c}Not active; no inhibition was observed at test compound concentrations of up to 100 μM.

biological activities expressed as IC$_{50}$ values are listed, all the compounds proved to inhibit the target enzyme, exhibiting potency levels in the submicromolar to micromolar range. The benzyloxy-substituted compound 5a (IC$_{50}$ = 0.99 ± 0.02 μM) displayed a remarkable inhibitory activity, showing a 36-fold enhancement in potency with respect to that of VS hit 1 (IC$_{50}$ = 35.6 ± 1.8 μM). Moving from 5a, we then added either electron-donating or electron-withdrawing groups to the pendant ring, to explore their contribution to a fruitful interaction with the binding site of the enzyme. While the presence of a methoxy substituent, as in 5c (IC$_{50}$ = 4.52 ± 0.19 μM), or a bromo atom, as in 5f (IC$_{50}$ = 7.36 ± 0.37 μM), slightly decreased the inhibitory efficacy of the resulting compounds, the insertion of a methyl group (5b; IC$_{50}$ = 0.83 ± 0.03 μM), a fluoro atom (5d; IC$_{50}$ = 0.82 ± 0.02 μM), or a chloro atom (5e; IC$_{50}$ = 0.92 ± 0.04 μM), in the same position

of the ring, left essentially unaltered the potency of the unsubstituted compound, 5a. Similar results were also obtained in the presence of the bulkier trifluoromethyl group (5g; IC$_{50}$ = 1.94 ± 0.61 μM) or the concurrent presence of o-fluoro and p-bromo atoms (5h; IC$_{50}$ = 1.41 ± 0.05 μM), which turned out almost equipotent with parent 5a. Finally, the insertion of a nitro group at the *meta* position of the phenyl ring, as in 5i (IC$_{50}$ = 0.46 ± 0.01 μM), produced a 2-fold enhancement in potency with respect to that of parent compound 5a, confirming once more the fruitful contribution of this key substituent to the interaction with the amino acid residues surrounding the ALR2 active site.[26,46] To explore the effects of increasing the distance between the pendant benzyl group and the benzofuroxane core, a methylene spacer was inserted between these two key fragments, to obtain derivative 5j. This distance turned out to be a crucial element in determining the best spatial relationship between the pharmacophoric groups of the compounds. Actually, the lengthened derivative 5j, with an IC$_{50}$ value of 5.90 ± 0.25 μM, displayed a 6-fold reduction in inhibitory efficacy with respect to that of the shorter 5a. On the other hand, widening the secondary lipophilic area of the compounds turned out to be a successful strategy. Indeed, although the replacement of the pendant benzyl group with the naphthalen-2-yl core, as in 5k (IC$_{50}$ = 1.43 ± 0.04 μM), did not significantly affect the functional activity, the insertion of the benzothiazol-2-yl group resulted in a remarkable improvement in inhibitory efficacy as the resulting compound, 5m (IC$_{50}$ = 0.42 ± 0.01 μM), was shown to be the most active of the whole series.

All the synthesized compounds, 5a–k,m, were assayed for their ability to inhibit aldehyde reductase (EC 1.1.1.2, ALR1), a cytosolic enzyme closely related to ALR2. Besides sharing a high degree of structural homology, with 65% identical amino acid sequences, both the enzymes play a common detoxification role, being key components of the complex antioxidant cell defense system that ensures the efficient removal of toxic aldehydes arising from pathological conditions connected with oxidative stress, like diabetes. Accordingly, a clinically effective and safe ARI should be able to inhibit ALR2 selectively, leaving unaltered the detoxification role of ALR1. Tested at 100 μM, none of the synthesized benzofuroxanes showed appreciable ALR1 inhibitory activity (Table 1), thus proving to be completely selective inhibitors of ALR2.

The novel inhibitors were then tested for their ancillary NO donor properties. The amount of NO released was determined in a rat hepatic homogenate exploiting the Griess reaction, thus measuring nitrites obtained as oxidative products of NO. With the limited exception of 5d, 5h, and 5m, which turned out to be ineffective, and 5j, showing a modest efficacy, the remaining synthesized compounds all displayed relevant NO donor properties. As shown in Figure 2, the substitution pattern of the benzofuroxane core did not affect significantly the effectiveness of the test compounds, as the percentage of NO released by 5a–c, 5e–g, and 5i–k was almost the same. Actually, after incubation at 37 °C for 1 h, the extent of release covered a narrow range, going from 2 to 4%. Interestingly, all the active compounds released NO slowly and spontaneously. Indeed, differently from previously reported benzofuroxane derivatives, they did not require the assistance of a cysteine cofactor, generally exploited to induce the earliest bioactivation of this kind of compound, necessary for NO release.[47] Moreover, the contained amount of NO released by the test compounds, although smaller than the amount obtained with
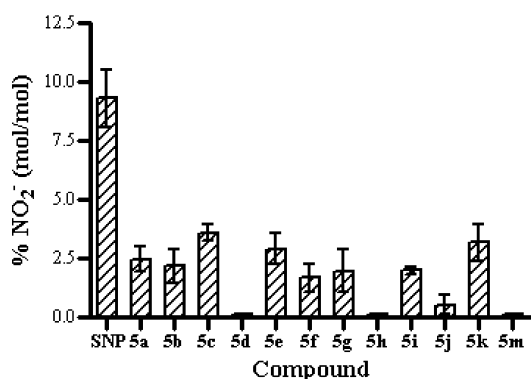
Figure 2. NO generation properties of benzofuroxane derivatives **5a–k,m**. Values are means ± the standard deviation. Each value is the mean of at last two different determinations, performed in triplicate.

the inorganic reference compound, sodium nitroprusside (SNP), represents a distinguishing quality. Actually, it may profitably control, or even prevent, hyperglycemia-induced vascular complications without posing the risks of toxicity and tolerance, often arising from NO donor compounds commonly available on the market.[33,48]

Finally, bearing in mind the crucial role played by oxidative stress in the pathogenesis of diabetic complications, we also investigated the newly synthesized compounds, **5a–k,m**, for their antioxidant properties. In particular, we examined their effects on hydroxyl radical-dependent lipoperoxidation induced in rat brain homogenate by the oxidant system Fe(III)/ascorbic acid, which initiates the Fenton reaction. For a proper comparison, the well-known antioxidant α-tocopherol was used as the reference standard. As reported in Figure 3, all the test compounds exhibited significant antioxidant properties, proving that the compounds reduce or even inhibit the production of thiobarbituric acid reactive substances (TBARS), an index of lipid peroxidation, when assayed at a final concentration of 100 μM. Compound **5a**, bearing a benzyloxy
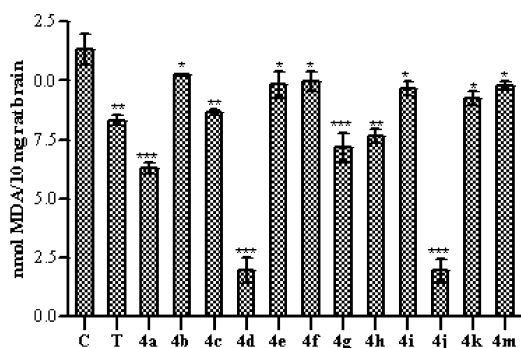

Figure 3. Effects of benzofuroxane derivatives, **5a–k,m**, and α-tocopherol on the production of thiobarbituric reactive substances (TBARS) in rat brain homogenate treated with the generating reactive oxygen species Fe(III)-ascorbic acid, expressed as nanomoles of malondialdehyde produced per 10 mg of wet weight rat brain. The basal value (rat brain homogenate) was 2.3 ± 0.39 nmol of TBARS/10 mg of wet weight rat brain ($n = 18$). Values are means ± the standard deviation. Each value is the mean of at least two different determinations, performed in triplicate. Absolute values were calculated by performing for each experiment a reference curve using 1,1,3,3-tetramethoxypropane. *$p < 0.05$; **$p < 0.01$; ***$p < 0.001$ [significant difference vs control group (rat brain homogenate with FeCl$_3$/ascorbic acid)]. C for control and T for α-tocopherol.

group, was significantly more effective than the reference α-tocopherol, inhibiting the production of TBARS by almost 50% when compared to the control. The addition of electron-donating substituents at the *para* position of the pendant phenyl ring, as for **5b,c**, slightly reduced the antioxidant efficacy, although it led to compounds that were still able to reduce the level of lipoperoxidation damage. Similar results were obtained through the insertion of electron-withdrawing groups at the same position of the ring, like in **5e–i**, as well as through the replacement of the phenyl group with the wider naphthalene, **5k**, and benzisothiazole, **5m**. On the other hand, the presence of a 4-fluorobenzyloxy substituent, as in **5d**, or a phenethoxy group, like in **5j**, gave rise to excellent scavenger properties, and the resulting compounds proved to significantly protect the rat brain homogenate from lipoperoxidation damage.

Interestingly, among the several promising compounds described here, benzyloxy derivative **5a** emerged for the excellent correlation between its high ALR2 inhibitory activity and significant NO donor and ROS scavenger properties, thus plainly proving the soundness of our choice to exploit suitably substituted benzofuroxanes as novel structures for development.

Molecular Modeling. To rationalize the achieved inhibitory activities of the newly identified ARIs, we performed docking experiments for compounds **5a–k,m** in the enzyme X-ray structure. These simulations were attained employing AutoDock4.2 (AD4) that, in our previous paper, successfully suggested **1** as an ALR2 inhibitor.[25] In the same study, the AD4 methodology was included in the so-called "in situ cross-docking" approach, to simultaneously address multiple ALR2 conformations.[49] Furthermore, given the well-known tautomerism of the benzofuroxane core, both tautomers of each compound, **5a–k,m**, were docked.

For all these calculations, AD4 predicted a general preference of the enzyme in recognizing only one of the two tautomers, namely the one bearing the aryloxy substituent at position 5 of the heterocyclic core. Moreover, as seen for parent **1**, the newly discovered ARIs were predicted to establish more stable complexes with the ALR2 conformation induced by the IDD594 ARI (Protein Data Bank entry 1US0).[50] In addition, for all these AD4 simulations, the lowest-energy binding conformation also represented the most populated cluster of binding poses, demonstrating good convergence behavior.

As seen for **5a**, in all the predicted lowest-energy ligand–ALR2 complexes, the benzofuroxane ring is placed in the ALR2 anion site while the pendant planar, lipophilic, and aromatic groups are lodged in the enzyme specificity pocket. In this cleft, the ligands are able to establish hydrophobic contacts with F122, L300, and Y309 and a π–π interaction with W111. In particular, among the benzyloxy derivatives, **5i** displayed the highest inhibitory potency against ALR2 because of the presence of the *m*-nitro substituent, which is able to enhance the π-stacking interactions with W111 and establish a H-bond interaction with T113 (Figure 4a). According to docking calculations, substitution of the benzyloxy moiety with the phenethoxy one, as in **5j**, negatively influences ALR2 recognition, and in the lowest-energy binding AD4 pose, the benzofuroxane moiety is placed in the specificity pocket while the terminal phenyl ring is lodged in the anion site (data not shown). This might explain why **5j** is less active than **5a**. On the other hand, substitution of the terminal phenyl ring with different aryl substituents generally confers better ALR2
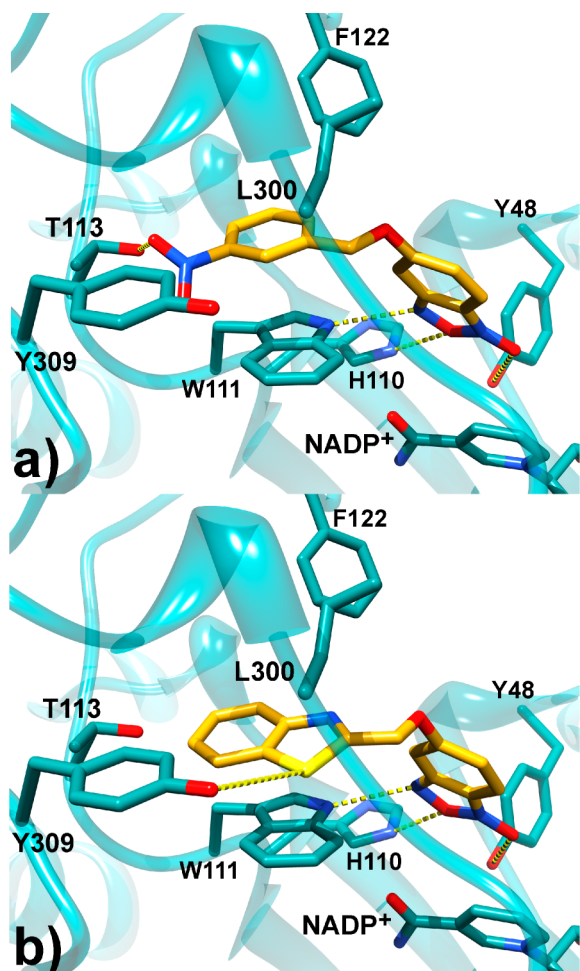
Figure 4. Docked conformations of **5i** (a) and **5m** (b) in the ALR2 structure. Hydrogens have been omitted for the sake of clarity. Ligand carbon atoms are colored yellow, and key binding site residues are displayed as blue sticks. Hydrogen bonds are represented by yellow dashed lines.

inhibitory potencies with the benzothiazol-2-yl ring derivative, **5m**, being the most active ARI of this series. In this case, the higher potency should be ascribed to the enhanced stacking interactions with W111 and to the presence of additional interactions in the specificity pocket, namely a H-bond with the side chain of Y309 and the nitrogen atom of the benzothiazol-2-yl ring (Figure 4b).

CONCLUDING REMARKS

Because of their multifactorial etiology, long-term diabetic complications, including the ones affecting the cardiovascular system, should be optimally treated with compounds capable of affecting simultaneously different biochemical pathways. In this work, we present a novel class of multi-effective compounds obtained by optimizing, in a suitably substituted benzofuroxane core, ALR2 inihibitory activity and selectivity with NO donor and antioxidant properties. Derivative **5a**, 4(5)-benzyloxyfuroxane, emerged as a new and viable lead, proving to merge submicromolar ALR2 inhibitory efficacy with both spontaneous NO releasing activity and significant hydroxyl radical scavenger ability. It clearly represents an original compound that, first in its field and different from the current clinical candidates, is intended to target diabetic complications taking advantage of a

multifactor approach. Further studies in animal models will prove its robustness as a prototypical drug candidate that can be exploited in preventing the onset and progression of hyperglycemia-induced cardiovascular diseases.

EXPERIMENTAL SECTION

Chemistry. Melting points were determined using a Reichert Köfler hot-stage apparatus and are uncorrected. Routine nuclear magnetic resonance spectra were recorded in DMSO-d_6 solutions on a Varian Gemini 200 spectrometer operating at 200 MHz. Mass spectra were obtained on a Hewlett-Packard 5988 A spectrometer using a direct injection probe and an electron beam energy of 70 eV. Evaporation was performed in vacuo (rotary evaporator). Analytical TLC was conducted on Merck 0.2 mm precoated silica gel aluminum sheets (60 F-254). The purity of the target inhibitors, **5a–k,m**, was determined by HPLC analysis, using a Merck Hitachi D-7000 liquid chromatograph (UV detection at 242 nm) and a Discovery C18 column (250 mm × 4.6 mm, 5 μm, Supelco), with a gradient of 40% water and 60% methanol and a flow rate of 1.4 mL/min. All the compounds showed percent purity values of ≥95%. 4-Amino-3-nitrophenol, 2-aminothiophenol, 2-(bromoethyl)benzene, 2-(bromomethyl)naphthalene, and the suitably substituted benzyl halide, used to obtain the target inhibitors, were from Alfa Aesar, Aldrich, and Fluka.

General Procedure for the Synthesis of 4-(4-Substituted benzyloxy)-2-nitrobenzenamines, 3a–l. A suspension of 4-amino-3-nitrophenol **2** (154.1 mg, 1.00 mmol) and the appropriate alkyl halide (1.10 mmol) in DMF was allowed to react at 90 °C in the presence of potassium carbonate (152.0 mg, 1.10 mmol) until the starting materials disappeared. Once the reaction was complete (TLC analysis, 7/3 petroleum ether/AcOEt, 60–80 °C), the mixture was concentrated to dryness and crushed ice was added. The resulting solid was collected and purified by recrystallization from the appropriate solvent, to obtain the title compound as red needles (Tables 1 and 2 of the Supporting Information).

Synthesis of 4-[(Benzo[*d*]thiazol-2-yl)methoxy]-2-nitrobenzenamine, 3m. A solution of 2-(4-amino-3-nitrophenoxy)acetonitrile (193.2 mg, 1.00 mmol), **3l**, and *o*-aminothiophenol (0.12 mL, 1.00 mmol) in 5 mL of anhydrous ethanol was refluxed while being stirred until the starting materials disappeared (2 h, TLC analysis, 7/3 petroleum ether/AcOEt, 60–80 °C). After the mixture had cooled, the resulting solid was collected by filtration and purified by recrystallization from ethanol (Tables 1 and 2 of the Supporting Information).

General Procedure for the Synthesis of 1-Azido-4-(4-substituted-benzyloxy)-2-nitrobenzenes and 2-[(4-Azido-3-nitrophenoxy)methyl]benzo[*d*]thiazole, 4a,b,d–k,m. A solution of sodium nitrite (172.5 mg, 2.50 mmol) in 2.0 mL of water was added dropwise to an ice-cold solution of the appropriate amine, **3a,b,d–k,m** (1.00 mmol), in concentrated hydrochloric acid. The resulting solution was stirred at 0 °C for 15 min, and then sodium azide (130.0 mg, 2.00 mmol) in 1.0 mL of water was added and the reaction mixture allowed to react overnight at room temperature. The target compound separated as a yellow solid, which was collected by filtration and purified by recrystallization (Tables 3 and 4 of the Supporting Information).

General Procedure for the Synthesis of 5(6)-Substituted Benzofuroxane Derivatives, 5a,b,d–k,m. A solution of the appropriate azide, **4a,b,d–k,m** (1.00 mmol), in 0.5 mL of acetic acid was heated under reflux until the starting material disappeared (TLC analysis, 7/3 toluene/CH$_2$Cl$_2$). The crude was poured into crushed ice, and the solid obtained, collected by filtration, was purified by recrystallization from the suitable solvent to give the target comounds, **5a,b,d–k,m**, as a mixture of tautomers (Tables 5 and 6 of the Supporting Information).

5(6)-(4-Methoxybenzyloxy)benzofuroxane, 5c. A solution of sodium hypochlorite (6–14%) was added dropwise to an ice-cold suspension of 4-(4-methoxybenzyloxy)-2-nitrobenzenamine, **3c** (274.1 mg, 1.00 mmol), and KOH (67.34 mg, 1.20 mmol) in anhydrous EtOH. Once the addition was complete, a yellow solid separated,

which was collected by filtration, washed with water, and recrystallized from the suitable solvent, to give target **5c** as a mixture of tautomers (Tables 5 and 6 of the Supporting Information).

Biological Materials and Methods. Assays were realized by exploiting adult Sprague-Dawley albino rats (body weights of 250−300), supplied by Harlan Nossan. Aldose reductase (ALR2) and aldehyde reductase (ALR1) were isolated and purified from rat lens and kidney, respectively, following a previously described protocol.[26] Pyridine coenzyme, D,L-glyceraldehyde, and sodium D-glucuronate were from Sigma-Aldrich. Epalrestat was obtained from Haorui Pharma-Chem Inc. All other chemicals were of reagent grade.

Enzymatic Assays. The activity of the two test enzymes was determined spectrophotometrically by monitoring the change in absorbance at 340 nm, which is due to the oxidation of NADPH catalyzed by ALR2 and ALR1. The change in pyridine coenzyme concentration per minute was determined using a Beckman DU-64 kinetics software program (Solf Pack TM Module).

ALR2 activity was assayed at 30 °C in a reaction mixture containing 0.25 mL of 10 mM D,L-glyceraldehyde, 0.25 mL of 0.104 mM NADPH, 0.25 mL of 0.1 M sodium phosphate buffer (pH 6.2), 0.1 mL of enzyme extract, and 0.15 mL of deionized water in a total volume of 1 mL. All these reagents, except D,L-glyceraldehyde, were incubated at 30 °C for 10 min; the substrate was then added to start the reaction, which was monitored for 5 min. Enzyme activity was calibrated by diluting the enzymatic solution to obtain an average reaction rate of 0.011 ± 0.0010 absorbance unit/min for the sample.

ALR1 activity was determined at 37 °C in a reaction mixture containing 0.25 mL of 20 mM sodium D-glucuronate, 0.25 mL of 0.12 mM NADPH, 0.25 mL of a dialyzed enzymatic solution, and 0.25 mL of 0.1 M sodium phosphate buffer (pH 7.2) in a total volume of 1 mL. The enzyme activity was calibrated by diluting the dialyzed enzymatic solution to obtain an average reaction rate of 0.015 ± 0.0010 absorbance unit/min for the sample.

Enzymatic Inhibition. The inhibitory activity of the newly synthesized compounds against ALR2 and ALR1 was assayed by adding 0.1 mL of the inhibitor solution to the reaction mixture described above. All the inhibitors were solubilized in water, and the solubility was facilitated by the addition of a small quantity of DMSO. To correct for the nonenzymatic oxidation of NADPH and for absorption by the compounds tested, a reference blank containing all the assay components listed above except the substrate was prepared. The inhibitory effect of the new derivatives was routinely estimated at a concentration of 10^{-4} M. Those compounds found to be active were tested at additional concentrations between 10^{-5} and 10^{-7} M. The determination of the IC_{50} values was performed by linear regression analysis of the log-dose response curve, which was generated using at least four concentrations of the inhibitor causing between 20 and 80% inhibition, with three replicates at each concentration. The 95% confidence limits (95% CL) were calculated from t values for $n - 2$, where n is the total number of determinations.

Quantitative Nitrite Detection in Rat Liver Homogenate. The NO releasing activity of test compounds, **5a−k,m**, was evaluated on the rat liver homogenate, obtained according to a previously reported procedure described by Kozlov et al. with slight modifications.[51] Liver was quickly removed, cut into small pieces, and washed with ice-cold sucrose buffer [100 mM K_2HPO_4, 1 mM EDTA, 1.15% (p/v) KCl, 0.25 M sucrose, and 0.1% EtOH (pH 7.4)] to remove blood. After being dried with paper, liver was weighted, suspended in the same buffer, added in a ratio of 1/6 (liver/buffer, w/v), and homogenized with Glass-Potter. The homogenate so obtained was filtered through three layers of surgical gauze and centrifuged for 10 min at 600g and 0 °C to pellet the nuclear fraction. The resulting supernatant, containing the mitochondrial, microsomal, and cytoplasmic fractions, was exploited to assess the NO donor properties of the test compounds; 200 μL of the filtrate was mixed with 300 μL of water and 500 μL of Griess reagent, containing 4% sulfanilamide and 0.2% naphthylethylendiamine dihydrochloride in 10% phosphoric acid, in the presence or absence of test compounds, at a concentration of 10^{-4} M. After incubation at 37 °C for 1 h, the amount of NO released was determined spectrophotometrically by measuring at 543 nm the

concentration of NO with a Perkin-Elmer Lambda instrument. The detected nitrites were evaluated as the oxidative products of nitric oxide by Griess reaction. Results are expressed as the percentage of NO_2^- (moles per mole) determined with respect to compound added (Figure 2).

Thiobarbituric Acid Reagent Substance (TBARS) Assay. Freshly isolated rat brain was homogenized in 10% (w/v) phosphate buffer (pH 7.4); 20 μM $FeCl_3$ and 100 μM ascorbic acid (final concentrations) were added to 100 μL of rat brain homogenate, in the absence or presence of the test compounds or reference scavenger molecules, and were diluted to a volume of 1 mL with phosphate buffer (pH 7.4). Samples were incubated for 30 min at 37 °C in a water bath while being slightly stirred and were then mixed with 0.5 mL of thiobarbituric acid [1% (w/v) in 0.05 N NaOH] and 0.5 mL of 25% (v/v) HCl. The mixture was boiled for 10 min, and after it had cooled in an ice-cold water bath, extraction was performed with 3 mL of n-butanol. After liquid phase separation (centrifugation at 2000g for 10 min), the absorbance of the pink organic phase was spectrophotometrically evaluated at 532 nm, and TBARS was expressed as nanomoles of malondialdehyde (MDA) per 10 mg of rat brain tissue (wet weight), using a curve with 1,1,3,3-tetramethoxypropane as the standard reference[27] (Figure 3).

Docking Studies. Structures of human ALR2 in complex with IDD594, sorbinil, and tolrestat were obtained from the Protein Data Bank (entries 1US0, 2FZD, and 2PDK, respectively). To add hydrogen to the structures mentioned above, MolProbity, an online tool for the validation and correction of protein structures, was used. To prepare the receptor for the docking procedure, proteins were all superimposed using their Cα atoms, and a subsite was selected having a radius of 12 Å from ligand. Residues not enclosed in such a selection were removed. The three subsites (derived from 1US0, 2FZD, and 2PDK) were then saved in a single file in which, while 1US0 was kept fixed, 2FZD and 2PDK were linearly aligned along the x-axis. In this step, to avoid docking results across the border of two adjacent subsites, the translation of 2FZD and 2PDK (−25 and 25 Å, respectively) was specified so that a partial overlap between subsites was present. After being removed from the prepared construct water molecules, all nonpolar hydrogens were merged to the parent carbon atoms. Then, all atom values were generated automatically through the GUI called AutoDockTools (ADT).[52] Grids were then generated for all the ligand atom types sufficient to describe all atoms in the selected database with the help of AutoGrid4,[53] using a grid spacing of 0.5 Å. The grid was centered on the 1US0 active site and had dimensions of 63 Å × 24 Å × 25 Å, which was sufficiently large to include the entire construct.

Ligand files were constructed employing the Builder tool and generated with the Ligprep module within the Maestro suite. Partial ligand charges and ligand electrostatic potentials were calculated by means of the Jaguar suite[54] within the Schrödinger package and mapped onto its electron density. The isovalue of 0.0004 electron/Bhor3 was chosen for the definition of the density surface, while the electrostatic potential was computed using LACVP* and 6-31G* basis sets with a scale of −0.0551 (red) to 0.0619 hartree (blue). The LACVP* basis set uses the standard 6-31G* basis set for light elements and the LAC pseudopotential (effective core potential for inner electrons) for the Br atom.[55]

All the ligands were then converted in the AutoDock4 format file (.pdbqt). For each ligand, 50 separate docking calculations were performed. Each docking calculation consisted of 10 million energy evaluations using the Lamarckian genetic algorithm local search (GALS) method. The GALS method evaluates a population of possible docking solutions and propagates the most successful individuals from each generation into the subsequent generation of possible solutions. A low-frequency local search according to the method of Solis and Wets is applied to docking trials to ensure that the final solution represents a local minimum. All dockings described in this paper were performed with a population size of 150, and 300 rounds of Solis and Wets local search were applied.

Hydrated Docking Procedure. The same parameters were also used for explicitly considering water molecules during docking

calculations of **5a**. In this procedure,[41] the ligand was hydrated using the wet.py suite, an additional grid map was calculated for the water molecules using the mapwater.py suite while, docking results were processed using the dry.py suite. All images of complexes were rendered employing UCSF Chimera.[56]

■ ASSOCIATED CONTENT

Ⓢ Supporting Information
Physical, spectral, and purity data of compounds described (Tables 1−7) and additional molecular modeling figures. This material is available free of charge via the Internet at http://pubs.acs.org.

■ AUTHOR INFORMATION

Corresponding Author
*C.L.M.: telephone, (+)390502219593; e-mail, concettina.lamotta@farm.unipi.it. L.M.: telephone, (+)39081679899; e-mail, luciana.marinelli@unina.it.

Notes
The authors declare no competing financial interest.

■ ABBREVIATIONS USED

ALR2, aldose reductase; AKR, aldo-keto reductase; NADPH, β-nicotinamide adenine dinucleotide phosphate, reduced form; NADP$^+$, β-nicotinamide adenine dinucleotide phosphate; ROS, reactive oxygen species; PKC, protein kinase C; ARIs, aldose reductase inhibitors; VS, virtual screening; NO, nitric oxide; TBARS, thiobarbituric acid reagent substance

■ REFERENCES

(1) Wild, S.; Roglic, G.; Green, A.; Sicree, R.; King, H. Global prevalence of diabetes: Estimates for the year 2000 and projections for 2030. *Diabetes Care* **2004**, *27*, 1047−1053.

(2) Zimmet, P. Z.; Alberti, K. G.; Shaw, J. Global and societal implications of the diabetes epidemic. *Nature* **2001**, *414*, 782−787.

(3) van Dieren, S.; Beulens, J. W.; van der Schouw, Y. T.; Grobbee, D. E.; Neal, B. The global burden of diabetes and its complications: An emerging pandemic. *European Journal of Cardiovascular Prevention and Rehabilitation* **2010**, *17*, S3−S8.

(4) International Diabetes Federation. *Diabetes Atlas*, 5th ed. (http://www.idf.org/diabetesatlas).

(5) Grundy, S. M.; Benjamin, I. J.; Burke, G. L.; Chait, A.; Eckel, R. H.; Howard, B. V.; Mitch, W.; Smith, S. C., Jr.; Sowers, J. R. Diabetes and cardiovascular disease: A statement for healthcare professionals from the American Heart Association. *Circulation* **1999**, *100*, 1134−1146.

(6) Brownlee, M. Biochemistry and molecular cell biology of diabetic complications. *Nature* **2001**, *414*, 813−820.

(7) Wiernsperger, N. F. Oxidative stress as a therapeutic target in diabetes: Revisiting the controversy. *Diabetes Metab.* **2003**, *29*, 579−585.

(8) Purves, T.; Middlemas, A.; Agthon, S.; Jude, E. B.; Boulton, A. J.; Fernyhough, P.; Tomlinson, D. R. A role for mitogen-activated protein kinases in the etiology of diabetic neuropathy. *FASEB J.* **2001**, *15*, 2508−2514.

(9) Williamson, J. R.; Chang, K.; Frangos, M.; Hasan, K. S.; Ido, Y.; Kawamura, T.; Nyengaard, J. R.; van der Enden, M.; Kilo, C.; Tilton, R. G. Hyperglycemic pseudohypoxia and diabetic complications. *Diabetes* **1993**, *42*, 801−813.

(10) Petrash, J. M. All in the family: Aldose reductase and closely related aldo-keto reductases. *Cell. Mol. Life Sci.* **2004**, *61*, 737−749.

(11) Tang, W. H.; Martin, K. A.; Hwa, J. Aldose reductase, oxidative stress, and diabetic mellitus. *Front. Pharmacol.* **2012**, *3*, 1−8.

(12) Chung, S. S.; Chung, S. K. Genetic analysis of aldose reductase in diabetic complications. *Curr. Med. Chem.* **2003**, *10*, 1375−1387.

(13) Asano, T.; Saito, Y.; Kawakami, M.; Yamada, N.; Fidarestat Clinical Pharmacology Study Group. Fidarestat (SNK-860), a potent aldose reductase inhibitor, normalizes the elevated sorbitol accumulation in erythrocytes of diabetic patients. *J. Diabetes Complications* **2002**, *16*, 133−138.

(14) Bril, V.; Hirose, T.; Tomioka, S.; Buchanan, R.; The Ranirestat Study Group. Ranirestat for the management of diabetic sensorimotor polyneuropathy. *Diabetes Care* **2009**, *32*, 1256−1260.

(15) Ramirez, M. A.; Borja, N. L. Epalrestat: An aldose reductase inhibitor for the treatment of diabetic neuropathy. *Pharmacotherapy* **2008**, *28*, 646−655.

(16) The Aldose Reductase Inhibitor-Diabetes Complications Trial Study Group. Short report: Treatment long-term clinical effects of epalrestat, an aldose reductase inhibitor, on progression of diabetic neuropathy and other microvascular complications: Multivariate epidemiological analysis based on patient background factors and severity of diabetic neuropathy. *Diabetes Medicine* **2012**, DOI: 10.1111/j.1464-5491.2012.03684.x.

(17) Reddy, A. B.; Ramana, K. V. Aldose reductase inhibition: Emerging drug target for the treatment of cardiovascular complications. *Recent Pat. Cardiovasc. Drug Discovery* **2010**, *5*, 25−32.

(18) Ramasamy, R.; Goldberg, I. J. Aldose reductase and cardiovascular diseases, creating human-like diabetic complications in an experimental model. *Circ. Res.* **2010**, *14*, 1449−1458.

(19) Gleissner, C. A.; Sanders, J. M.; Nadler, J.; Ley, K. Upregulation of aldose reductase during foam cell formation as possible link among diabetes, hyperlipidemia, and atherosclerosis. *Arterioscler., Thromb., Vasc. Biol.* **2008**, *28*, 1137−1143.

(20) Sellers, D. J.; Chess-Williams, R. The effects of streptozotocin-induced diabetes and aldose reductase inhibition with sorbinil, on left and right atrial function in the rat. *J. Pharm. Pharmacol.* **2000**, *52*, 687−694.

(21) Heather, L. C.; Clarke, K. Metabolism, hypoxia and the diabetic heart. *J. Mol. Cell. Cardiol.* **2011**, *50*, 598−605.

(22) Srivastava, S. K.; Yadav, U. C.; Reddy, A. B.; Saxena, A.; Tammali, R.; Shoeb, M.; Ansari, N. H.; Bhatnagar, A.; Petrash, M. J.; Srivastava, S.; Ramana, K. V. Aldose reductase inhibition suppresses oxidative stress-induced inflammatory disorders. *Chem.-Biol. Interact.* **2011**, *191*, 330−338.

(23) Ramunno, A.; Cosconati, S.; Sartini, S.; Maglio, V.; Angiuoli, S.; La Pietra, V.; Di Maro, S.; Giustiniano, M.; La Motta, C.; Da Settimo, F.; Marinelli, L.; Novellino, E. Progresses in the pursuit of aldose reductase inhibitors: The structure-based lead optimization step. *Eur. J. Med. Chem.* **2012**, *51*, 216−226.

(24) Ottanà, R.; Maccari, R.; Giglio, M.; Del Corso, A.; Cappiello, M.; Mura, U.; Cosconati, S.; Marinelli, L.; Novellino, E.; Sartini, S.; La Motta, C.; Da Settimo, F. Identification of 5-arylidene-4-thiazolidinone derivatives endowed with dual activity as aldose reductase inhibitors and antioxidant agents for the treatment of diabetic complications. *Eur. J. Med. Chem.* **2011**, *46*, 2797−2806.

(25) Cosconati, S.; Marinelli, L.; La Motta, C.; Sartini, S.; Da Settimo, F.; Olson, A. J.; Novellino, E. Pursuing aldose reductase inhibitors through in situ cross-docking and similarity-based virtual screening. *J. Med. Chem.* **2009**, *52*, 5578−5581.

(26) La Motta, C.; Sartini, S.; Salerno, S.; Simorini, F.; Taliani, S.; Marini, A. M.; Da Settimo, F.; Marinelli, L.; Limongelli, V.; Novellino, E. Acetic acid aldose reductase inhibitors bearing a five-membered heterocyclic core with potent topical activity in a visual impairment rat model. *J. Med. Chem.* **2008**, *51*, 3182−3193.

(27) La Motta, C.; Sartini, S.; Mugnaini, L.; Simorini, F.; Taliani, S.; Salerno, S.; Marini, A. M.; Da Settimo, F.; Lavecchia, A.; Novellino, E.; Cantore, M.; Failli, P.; Ciuffi, M. Pyrido[1,2-*a*]pyrimidin-4-one derivatives as a novel class of selective aldose reductase inhibitors exhibiting antioxidant activity. *J. Med. Chem.* **2007**, *50*, 4917−4927.

(28) Da Settimo, C.; Primofiore, G.; La Motta, C.; Sartini, S.; Taliani, S.; Simorini, F.; Marini, A. M.; Lavecchia, A.; Novellino, E.; Boldrini, E. Naphtho[1,2-*d*]isothiazole acetic acid derivatives as a novel class of selective aldose reductase inhibitors. *J. Med. Chem.* **2005**, *48*, 6897−6907.

(29) Da Settimo, F.; Primofiore, G.; La Motta, C.; Salerno, S.; Novellino, E.; Greco, G.; Lavecchia, A.; Laneri, S.; Boldrini, E. Spirohydantoin derivatives of thiopyrano[2,3-*b*]pyridin-4(4*H*)-one as potent in vitro and in vivo aldose reductase inhibitors. *Bioorg. Med. Chem.* **2005**, *13*, 491−499.

(30) Da Settimo, F.; Primofiore, G.; Da Settimo, A.; La Motta, C.; Simorini, F.; Novellino, E.; Greco, G.; Lavecchia, A.; Boldrini, E. Novel, highly potent aldose reductase inhibitors: Cyano(2-oxo-2,3-dihydroindol-3-yl)acetic acid derivatives. *J. Med. Chem.* **2003**, *46*, 1419−1428.

(31) Da Settimo, F.; Primofiore, G.; Da Settimo, A.; La Motta, C.; Taliani, S.; Simorini, F.; Novellino, E.; Greco, G.; Lavecchia, A.; Boldrini, E. [1,2,4]Triazino[4,3-*a*]benzimidazole acetic acid derivatives: A new class of selective aldose reductase inhibitors. *J. Med. Chem.* **2001**, *44*, 4359−4369.

(32) Gosh, P. B.; Everitt, B. J. Furazanobenzofuroxan, furazanobenzothiadiazole, and their N-oxides. A new class of vasodilator drugs. *J. Med. Chem.* **1974**, *17*, 203−206.

(33) Sankaranarajanan, A. Use of benzofuroxan derivatives in treating angina pectoris. U.S. Patent 6,232,331B1, 2001.

(34) Gosh, P. B.; Ternai, B.; Whitehouse, M. Benzofurazans and benzofuroxans: Biochemical and pharmacological properties. *Med. Res. Rev.* **1981**, *1*, 159−187.

(35) Pacher, P.; Beckman, J. S.; Liaudet, L. Nitric oxide and peroxynitrite in health and disease. *Physiol. Rev.* **2007**, *87*, 315−424.

(36) Fioramonti, X.; Song, Z.; Vazirani, R. P.; Beuve, A.; Routh, V. H. Hypothalamic nitric oxide in hypoglycemia detection and counter-regulation: A two-edged sword. *Antioxid. Redox Signaling* **2011**, *14*, 505−517.

(37) Srivastava, S.; Tammali, R.; Chandra, D.; Greer, D. A.; Ramana, K. V.; Bhatnagar, A.; Srivastava, S. K. Regulation of lens aldose reductase activity by nitric oxide. *Exp. Eye Res.* **2005**, *81*, 664−672.

(38) Ramana, K. V.; Chandra, D.; Srivastava, S.; Bhatnagar, A.; Srivastava, S. K. Nitric oxide regulates the polyol pathway of glucose metabolism in vascular smooth muscle cells. *FASEB J.* **2003**, *17*, 417−425.

(39) Srivastava, S. K.; Ramana, K. V.; Chandra, D.; Srivastava, S.; Bhatnagar, A. Regulation of aldose reductase and the polyol pathway activity by nitric oxide. *Chem.-Biol. Interact.* **2003**, *143−144*, 333−340.

(40) Chandra, D.; Jackson, E. B.; Ramana, K. V.; Kelley, R.; Srivastava, S. K.; Bhatnagar, A. Nitric oxide prevents aldose reductase activation and sorbitol accumulation during diabetes. *Diabetes* **2002**, *51*, 3095−3101.

(41) Forli, S.; Olson, A. J. A force field with discrete displaceable waters and desolvation entropy for hydrated ligand docking. *J. Med. Chem.* **2012**, *55*, 623−638.

(42) Oates, P. J.; Mylari, B. L. Aldose reductase inhibitors: Therapeutic implications for diabetic complications. *Expert Opin. Invest. Drugs* **1999**, *8*, 2095−2119.

(43) Ruggeri, S. G.; Bill, D. R.; Bourassa, D. E.; Castaldi, M. J.; Houck, T. L.; Brown Ripin, D. H.; Wein, L.; Weston, N. Safety vs efficiency in the development of a high-energy compound. *Org. Process Res. Dev.* **2003**, *7*, 1043−1047.

(44) Leyva, S.; Castanedo, V.; Leyva, E. Synthesis of novel fluorobenzofuroxans by oxidation of anilines and thermal cyclization of arylazides. *J. Fluorine Chem.* **2003**, *121*, 171−175.

(45) Dyall, L. K. Oxidative cyclizations. VII. Cyclization of 2-substituted anilines with alkaline hypohalite. *Aust. J. Chem.* **1984**, *37*, 2013−2026.

(46) Steuber, H.; Heine, A.; Klebe, G. Structural and thermodynamic study on aldose reductase: Nitro-substituted inhibitors with strong enthalpic binding contribution. *J. Mol. Biol.* **2007**, *368*, 618−638.

(47) Medana, C.; Di Stilo, A.; Visentin, S.; Fruttero, R.; Gasco, A.; Ghigo, D.; Bosia, A. NO donor and biological properties of different benzofuroxans. *Pharm. Res.* **1999**, *16*, 956−960.

(48) Guo, Y.; Jones, W. K.; Xuan, Y. T.; Tang, X. L.; Bao, W.; Wu, W. J.; Han, H.; Laubach, V. E.; Ping, P.; Yang, Z.; Qiu, Y.; Bolli, R. Tha late phase of ischemic preconditioning is abrogated by targeted disruption of the inducible NO synthase gene. *Proc. Natl. Acad. Sci. U.S.A.* **1999**, *96*, 11507−11512.

(49) Sotriffer, C. A.; Dramburg, I. "In situ cross-docking" to simultaneously address multiple targets. *J. Med. Chem.* **2005**, *48*, 3122−3125.

(50) Howard, E. I.; Sanishvili, R.; Cachau, R. E.; Mitschler, A.; Chevrier, B.; Barth, P.; Lamour, V.; Van Zandt, M.; Sibley, E.; Bon, C.; Moras, D.; Schneider, T. R.; Joachimiak, A.; Podjarny, A. *Proteins* **2004**, *55*, 792−804.

(51) Kozlov, A. V.; Dietrich, B.; Nohl, H. Various intracellular compartments cooperate in the release of nitric oxide from glycerol trinitrate in liver. *Br. J. Pharmacol.* **2003**, *139*, 989−997.

(52) Sanner, M. F. Python: A programming language for software integration and development. *J. Mol. Graphics Modell.* **1999**, *17*, 57−61.

(53) (a) Huey, R.; Morris, G. M.; Olson, A. J.; Goodsell, D. S. A semiempirical free energy force field with charge-based desolvation. *J. Comput. Chem.* **2007**, *28*, 1145−1152. (b) Cosconati, S.; Forli, S.; Perryman, A. L.; Harris, R.; Goodsell, D. S.; Olson, A. J. Virtual Screening with AutoDock: Theory and Practice. *Expert Opin. Drug Discovery* **2010**, *5*, 597−607.

(54) *Jaguar 4.1*; Schrödinger, Inc.: Portland, OR, 2000.

(55) For details regarding the LACVP* basis set, see the *Jaguar 4.1* manual.

(56) Pettersen, E. F.; Goddard, T. D.; Huang, C. C.; Couch, G. S.; Greenblatt, D. M.; Meng, E. C.; Ferrin, T. E. UCSF Chimera: A visualization system for exploratory research and analysis. *J. Comput. Chem.* **2004**, *25*, 1605−1612.